

# Ultrasound biomicroscopic evaluation of anterior segment cysts as a risk factor for ocular hypertension and closure angle glaucoma

Abdurrahim Dusak<sup>1</sup>, Mehmet Baykara<sup>2</sup>, Guven Ozkaya<sup>3</sup>, Cuneyt Erdogan<sup>1</sup>, Hikmet Ozcetin<sup>2</sup>, Ercan Tuncel<sup>1</sup>

<sup>1</sup>Department of Radiology, School of Medicine, Uludag University, Bursa 16059, Turkey

<sup>2</sup>Department of Ophthalmology, School of Medicine, Uludag University, Bursa 16059, Turkey

<sup>3</sup>Department of Statistics, School of Medicine, Uludag University, Bursa 16059, Turkey

**Correspondence to:** Abdurrahim Dusak. Department of Radiology, School of Medicine, Uludag University, Gorukle Campus, Bursa 16059, Turkey. adusak@uludag.edu.tr

Received: 2013-04-16

Accepted: 2013-06-06

which can be determined by UBM.

• **KEYWORDS:** anterior-segment cyst; ocular hypertension, closed-angle glaucoma; intraocular pressure; ultrasound biomicroscopy

**DOI:10.3980/j.issn.2222-3959.2013.04.20**

Dusak A, Baykara M, Ozkaya G, Erdogan C, Ozcetin H, Tuncel E. Ultrasound biomicroscopic evaluation of anterior segment cysts as a risk factor for ocular hypertension and closure angle glaucoma. *Int J Ophthalmol* 2013;6(4):515-520

## Abstract

• **AIM:** To investigate the relationship between the ultrasound biomicroscopic (UBM) features of anterior-segment cysts (ASCs) and increased intraocular pressure (IOP) as a risk factor for closed-angle glaucoma (CAG).

• **METHODS:** Totally 24 eyes with recently diagnosed ASCs were divided into two groups. First group with ASC and ocular normotension ( $n=13$ ), second group with ASC and ocular hypertension ( $n=11$ ). An ophthalmologic examination, including tonometry, slit-lamp biomicroscopy (SLBM), gonioscopy, funduscopy, pentacam, and UBM, was performed. The features of the ASCs were compared with the IOP.

• **RESULTS:** ASCs were accurately diagnosed and delineated in 24 eyes using UBM. IOP was elevated in those ASCs with a secondary aetiology ( $P=0.027$ ), iridociliary location ( $P=0.006$ ), deformed shape ( $P=0.013$ ), increased size ( $P=0.001$ ) and elongated pupillary aperture ( $P=0.009$ ). However, the count ( $P=0.343$ ) of ASCs, anterior chamber depth (ACD;  $P=0.22$ ) and axial length (AL;  $P=0.31$ ) were not associated with ocular hypertension. Correlations were found between the IOP and ASC size ( $r=-0.712$ ;  $P=0.003$ ), anterior chamber angle (ACA;  $r=-0.985$ ;  $P<0.001$ ), angle opening area (AOA;  $r=0.885$ ;  $P<0.001$ ), angulation of iris ( $r=-0.776$ ,  $P<0.001$ ), and affected iris quadrant ( $r=-0.655$ ,  $P=0.002$ ).

• **CONCLUSION:** Ocular hypertension in some eyes with ASC might be associated with various mechanisms, including secondary aetiology, iridociliary location, deformed shape, increased size and elongated pupill,

## INTRODUCTION

Anterior-segment cysts (ASCs) are uncommon, usually non-pigmented small sacs arising from the posterior iris that may be diagnosed incidentally and which are classified as primary or secondary aetiology<sup>[1]</sup>. Primary ASCs are usually benign and slow growing; however, spontaneous involution can also occur<sup>[2]</sup>. Primary ASCs, including epithelial and stromal subtypes, are well-defined, contain anechoic fluid, and have moderately thin and hyperechoic walls<sup>[3]</sup>. Secondary ASCs result from the implantation of epithelial cells in the iris stroma due to penetrating trauma, surgery, uveitis, or the long-term use of miotic agents<sup>[4]</sup>. Secondary ASCs tend to be larger in size, thick-walled, and fluid-filled, including inflammatory debris. Such ASCs may cause impression distortion on the cornea, iris, or lens, leading to closure of the anterior-chamber angle (ACA) and angle opening area (AOA)<sup>[5,6]</sup>. Pupillary block is an uncommon complication, presenting with intermittent closed-angle glaucoma (CAG)<sup>[7]</sup>.

The clinical presentation of ASCs varies. Most are stable and asymptomatic<sup>[8]</sup>. However, they can occasionally cause complications, due to an increase in size and iris angulation, including closure of the ACA-AOA, narrowed pupillary aperture, corneal decompensation, iridocyclitis, uveitis, and glaucoma<sup>[9,10]</sup>. The flow of aqueous humour from the ciliary body to the trabecular meshwork through the pupillary aperture generates a normal intraocular pressure (IOP) of 10 to 20mmHg<sup>[11]</sup>. ASCs and their complications can be interrupted as a result of increased inflow, decreased outflow, or an elevated IOP<sup>[12,13]</sup>. Axial length (AL) and anterior

chamber depth (ACD) of eyes are increased in primary glaucoma<sup>[11]</sup>.

The management of ASCs varies in accordance with the related complications<sup>[5]</sup>. ASCs should be imaged in detail before surgery to determine their internal characteristics, to distinguish them from similar lesions, and to ascertain whether they involve the ciliary body, iris, lens, or cornea<sup>[14]</sup>. An increased IOP may be associated with the ultrasound biomicroscopic (UBM) features of ASCs, including the number, size, shape, location, and effect on adjacent tissue.

The purpose of this cross-sectional retrospective study was to evaluate the clinical manifestations and UBM features of ASCs for closed ACA-AOA with or without ocular hypertension (OHT). If characteristic UBM features could be identified, it would assist in making a diagnosis and permit a rational treatment approach based on the underlying mechanism.

### SUBJECTS AND METHODS

**Subjects** We investigated 24 eyes of consecutive patients (13 female) with recently diagnosed ASC, aged 19-78 ( $45.5 \pm 20.8$ ) years, who were referred our center to evaluate for increased IOP between 2006 and 2010. Patients with ASC and OHT ( $n=11$ ) or ocular normotension (ONT,  $n=13$ ) comprised two groups. All participants underwent a complete and detailed ocular examination, including ophthalmological and medical history, visual acuity, IOP, applanation tonometry, slit-lamp biomicroscopy (SLBM), and gonioscopy. Patients with acute uveitis, tumours, diabetes, those on medication, and those who had a poor UBM image quality were excluded. This study was approved by our Institutional Review Board. The participants provided informed consent in accordance with the principles of the Declaration of Helsinki.

**UBM** UBM was performed using a UBM (HF35-50 High Frequency Ultrasound; OTI Ophthalmic Technologies Inc., Kodiak Crescent, Toronto, ON, Canada). Topical proparacaine 0.1% (Alcaine; Alcon Laboratories, Fort Worth, TX, USA) was administered with the patients in the supine position. A scleral cup was inserted and filled with gel. It was applied with no pressure to the globe and no touching of the cornea to avoid measurement error. UBM images of the anterior segment were recorded. The procedure was applied in dim light without the Valsalva manoeuvre, and maintained fixation with the other eye<sup>[15,16]</sup>. The probe was moved perpendicularly on the eye and scanned radially according to the location of the ASC (Figure 1). UBM was evaluated for narrowing of the ACA-AOA. A single observer (Baykara M) performed all examinations, which were subsequently reassessed and graded by a second observer (Dusak A).

**Methods** UBM scans were transferred to a workstation. The following parameters were analysed for each eye. The ACA was measured for the largest ASC using radial scans. UBM images were obtained perpendicular to the ocular surface to

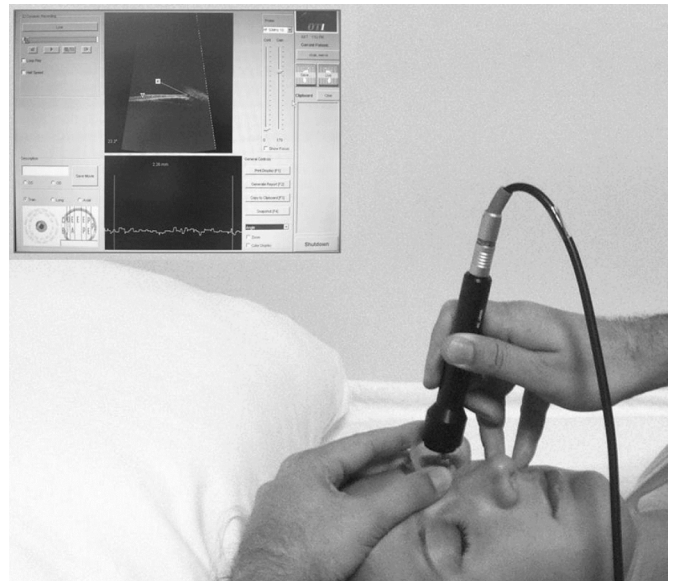


Figure 1 UBM was performed in the supine position.

avoid distorted images and non-reproducible ACA measurements. Each measurement was repeated three times, and the average value was taken. The UBM system provided the AL, ACD, ACA, AOA, and angulation of iris as linear and angular parameters. All calculations were performed using the integrated standard UBM software (OCTeval, ver. 1.1; 4Optics, Lubeck, Germany) system measured the cross-sectional images. The scleral spur was used as a reference point for the measurements<sup>[17]</sup>. The Van Herick grading system was used to assess the ACA-AOA<sup>[18,19]</sup>. The ACA was determined by two lines from the iridocorneal angle, as described by Pavlin<sup>[20]</sup>. The first line lay through the scleral spur along the internal border of the cornea, while the second lay parallel with one-third of the peripheral iris surface<sup>[21]</sup>. The AOA was measured as described by Console<sup>[22]</sup>. The area between the internal border of the cornea and the posterior surface of the iris from the scleral spur to a point 500 $\mu$ m away in the perpendicular direction was used to estimate the corneal thickness<sup>[23,24]</sup>. Iris convexity was determined as described by Potash<sup>[25]</sup>. Iris angulation was determined using lines extending from the greatest point to the periphery and centre of the iris<sup>[23]</sup>. Quadrant analysis of the iris was performed as described by Kumar<sup>[26]</sup>. Four quadrants were evaluated: nasal-temporal and superior-inferior.

All measurements were evaluated and analysed by the same trained investigator (Baykara M) in an unmasked manner, and were confirmed by a second expert (Dusak A) who was masked to image acquisition, patient history, and the first investigator. Inter-rater reliability was calculated using intraclass correlations (ICCs) between pairs of raters. The ICC was deemed satisfactory (0.961; 95% CI: 0.905-0.985). Agreement between the pentacam with the average raters UBM measurements was examined using Bland-Altman plots.

**Table 1 Baseline ophthalmological characteristics of the ASC groups**

Variables	All ASC	Patients with ASC and OHT	Controls with ASC and ONT	P
n	24	11	13	
a	41.5±19.3	42.5±19.3	39.6±21.4	0.43
F/M	13/11	7/6	6/5	0.61
IOP (mmHg)	18.0±3.7	24.0±3.4	14.4±3.1	0.001
ACA (A°)	23.8±6.3	18.8±5.3	27.3±4.6	0.001
AOA (mm <sup>2</sup> )	25.1±7.5	21.1±6.8	29.1±3.9	0.001
ACD (mm)	3.5±0.2	3.6±0.3	3.4±0.2	0.22
AL (mm)	23.4±1.0	23.5±1.1	23.4±1.1	0.31

Data are presented as mean ±SD. ASC: Anterior segment cyst; OHT: Ocular hypertension; ONT: Ocular normotension; IOP: Intraocular pressure; ACA: Anterior chamber angle; AOA: Angle opening area; ACD: Anterior-chamber depth; AL: Axial length.

**Statistical Analysis** Statistical tests were used to evaluate the relationship between the UBM features of the ASCs and the IOP. All parameters were classified as categorical. A Chi-square test was applied to analyse the variables. The Shapiro-Wilk test was used to check normality for continuous variables. Non-normal continuous variables were compared with the Mann-Whitney *U* test, for comparison of the IOP according to the UBM features of the ASCs. Correlations between variables were determined based on Pearson and Spearman correlation coefficients. All statistical analyses were performed using SPSS ver. 17.0 and MedCalc version 12.1.0.

**RESULTS**

Baseline characteristics were presented in Table 1. There was no significant difference in age ( $P=0.43$ ), gender ( $P=0.61$ ), ACD ( $P=0.22$ ), AL ( $P=0.31$ ) between the OHT and ONT groups. ACA ( $18.8\pm5.3$ ,  $27.3\pm4.6$ ;  $P=0.001$ ) was significantly lower in the OHT group than in the ONT group. Nineteen eyes had primary ASCs with thin walls and a sonolucent content. Five eyes had secondary ASCs due to trauma with a larger size, slightly thick walls, and a sonolucent appearance; one eye had a few free echogenic particles and septation. Of the ASCs, 2 were midzonal, 16 were iridociliary, and 6 were in the ciliary body. Fewer (less than three) ASCs were noted in 17 eyes and multiple (more than three) ACCs in 7 eyes (Figure 2). The midzonal ASCs tended to elongate anteriorly (Figure 3). However, the iridociliary ASCs tended to extend between the lens and iris posteriorly through the pupillary aperture (Figure 4). Secondary aetiology ( $P=0.027$ ), iridociliary location ( $P=0.006$ ), deformed shape ( $P=0.012$ ), increased size ( $P=0.001$ ), and extension through the pupillary aperture ( $P=0.009$ ) were significantly associated with OHT. In contrast, count ( $P=0.343$ ) of ASCs were not associated with the IOP (Table 2).

Iris convexity was absent in 5 eyes, increased mildly in 7 eyes, increased moderately in 8 eyes, and increased extremely in 4 eyes. Iris was affected in one quadrant in 8 eyes, two quadrant in 9 eyes, and three quadrant in 7 eyes. The ACA Van Herick grading was as follows: grade IV in 5

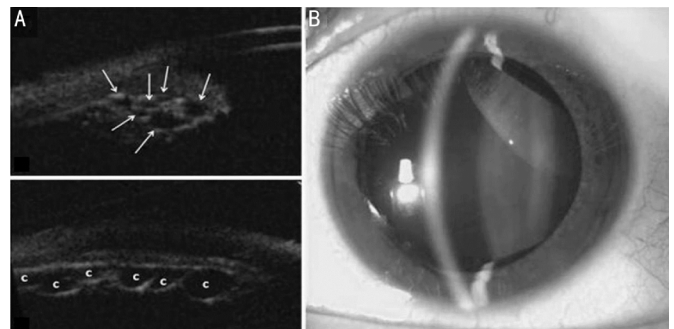


**Figure 2 A 39-year-old male with pseudo-plateau iris appearance with bilateral multiple iridociliary ASCs** Multi-directional UBM (A) and slit-lamp biomicroscopy (B) show multiple spherical and oval ASCs (arrows), ACA-ACD moderately open. IOP=20mmHg; c: ASC.

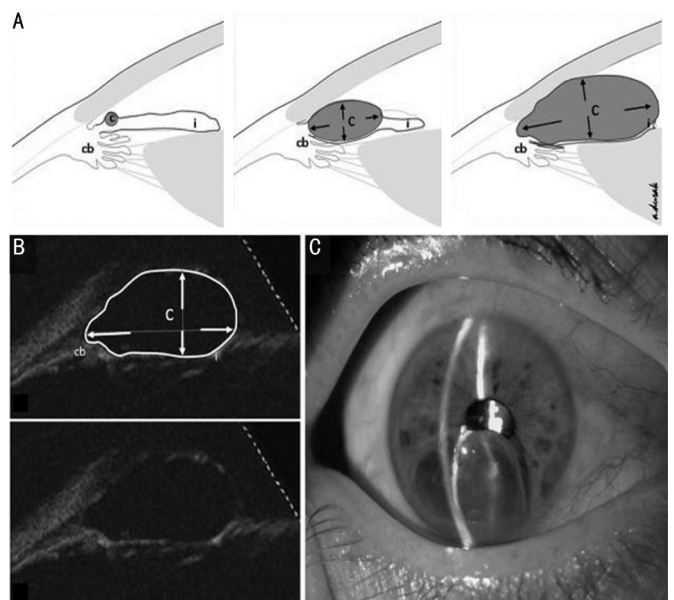


**Figure 3 A 67-year-old female with impressed midzonal single ASC** Schematic depicting (A), UBM (B) and slit-lamp biomicroscopy (C) of ASC growth anteriorly with centripetal expansion and becoming deformed, and show relationship between shape of ASC in growth (arrows) and closing of ACA-ACD, show pupillary narrowing, IOP=36mmHg, surgical cyst excision was applied. i: iris; cb: ciliary body; c: ASC.

eyes, grade III in 7 eyes, grade II in 8 eyes, and grade I in 4 eyes. Significant correlations were found between the IOP

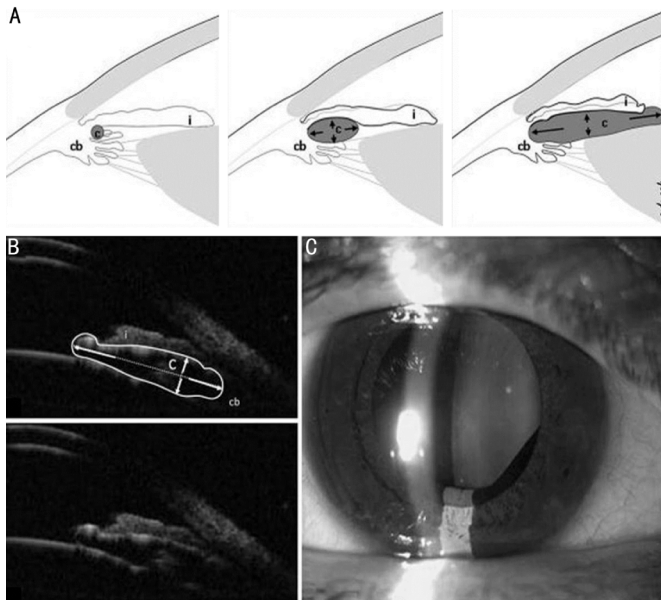


**Figure 4** A 39-year-old male with pseudo-plateau iris, bilateral iridociliary ASCs growth posteriorly. Schematic depicting (A), multi-directional UBM (B) and slit-lamp biomicroscopy (C): interrelationship between the shape of the ASC (arrows) and closing ACA-AOA shows single impressed iridociliary ASC with pupillary extension, IOP=31mmHg; c: ASC.

**Table 2** Association between ASC groups for UBM features of ASC

Parameters of ASC	Patients with ASC and OHT	Controls with ASC and OHT	<i>n</i> (%)	<i>P</i>
<b>Etiology</b>				
Primary	7 (29)	12 (50)		0.027
Secondary	4 (17)	1 (4)		
<b>Location</b>				
Midzonal	1 (4)	1 (4)		0.006
Iridociliary	10 (42)	6 (25)		
Ciliary body	0 (0)	6 (25)		
<b>Count</b>				
Fewer ( $\leq 3$ )	10 (42)	7 (29)		0.343
Multiple ( $>3$ )	1 (4)	6 (25)		
<b>Shape</b>				
Spherical	0 (0)	5 (21)		0.012
Oval	3 (13)	8 (33)		
Deformed	8 (33)	0 (0)		
<b>Size (mm<sup>2</sup>)</b>				
Small ( $<3$ )	0 (0)	6 (25)		0.001
Medium (4-9)	4 (17)	7 (29)		
Large ( $\geq 10$ )	7 (29)	0 (0)		
<b>Pupillary aperture</b>				
Open	3 (13)	13 (54)		0.009
Narrow	8 (33)	0 (0)		
<b>Angulation of iris</b>				
None	0 (0)	7 (29)		0.001
Minimal	2 (8)	5 (21)		
Moderate	5 (21)	1 (4)		
Significant	4 (17)	0 (0)		
<b>Affected iris quadrant</b>				
I (0° -90°)	2 (8)	8 (33)		0.002
II (90° -180°)	6 (25)	4 (17)		
III (180° -270°)	3 (13)	1 (4)		
IV (270° -360°)	0 (0)	0 (0)		
<b>Pupillary aperture</b>				
Open	3 (13)	13 (54)		0.009
Narrow	8 (33)	0 (0)		

Data are presented as number and percentage. ASC: Anterior segment cyst; UBM: Ultrasound biomicroscopy; OHT: Ocular hypertension; OHT: Ocular normotension.

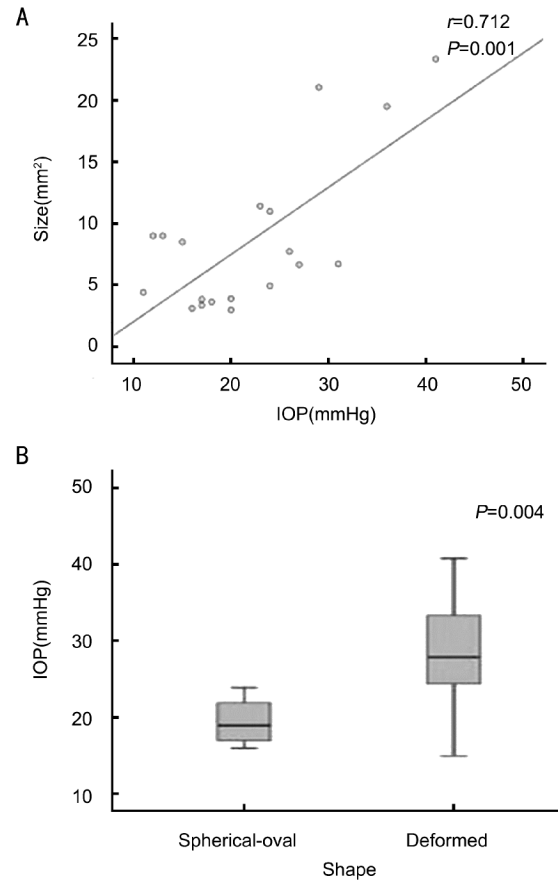


**Figure 5** Correlation between IOP and size of ASC, the distribution of IOP and shape of ASC. A: Correlation between IOP and size of ASC ( $r=0.712$ ;  $P=0.001$ ); B: Box plot showing the distribution of IOP and shape of ASC (spherical-oval and deformed appearance;  $P=0.004$ ).

and ACA ( $r=-0.985$ ;  $P<0.001$ ), AOA<sub>van Herick</sub> ( $r=-0.899$ ;  $P<0.001$ ), convexity ( $r=0.735$ ;  $P<0.001$ ), affected quadrant ( $r=0.814$ ,  $P<0.001$ ) of iris, and size of ASCs ( $r=0.648$ ;  $P=0.003$ ) (Figure 5).

**DISCUSSION**

We investigated a series of eyes with ASCs referred for an evaluation of CAG on their UBM features. We found that a secondary aetiology, iridociliary location, deformed shape, extended pupillary aperture, and increased size were significantly correlated with an OHT, and often had a closed ACA, consistent with previous findings. An increased IOP was not related to the number of ASC. Having an OHT was positively correlated with having an angulated, affected iris quadrant, and the Van Herick grade of the ASCs was negatively correlated with an increase in the IOP.

ASCs are stationary lesions that rarely progress and cause complications [1]. Epithelial ASCs are remarkably stable; stromal ASCs tend to enlarge and adhere to the iris due to epithelial cell desquamation and keratin and mucin production, creating a high colloidal osmotic pressure [10]. This might be due to rapid fluid inflow through the semipermeable ASC wall. Enlarging ASCs can become herniated into the pupillary aperture, resulting in closure of the visual axis [27].

An increase in IOP may be due to decreased outflow of the aqueous humour with an anteriorly dislocated iris or increased secretion and inflow of the aqueous humour due to the influence of the ASC on the ciliary body [28,29]. Additional complications of ASCs include uveitis, corneal oedema, and focal lens opacification [13,30]. A few studies have reported more severe complications, including nanophthalmos, buphthalmos, blindness, and loss of the eye [9,12]. The diagnosis of CAG requires assessment of the ACA-AOA and whether the trabecular meshwork is blocked [31]. The associations identified in this study between the UBM features of ASCs and increased IOP are useful because the management of ASCs could be changed by underlying closure of the ACA [28,32]. ASCs can become quite large and deformed in shape, and this is associated with the pressure in the inner and outer cysts [10,33]. A ring-shaped ASC has been reported, which filled the entire PC and was distended like an inner tube in the eye with increased IOP [27]. This suggests that the position of the growing ASC results from traction of the zonula in an iridociliary location. Continuing growth of the ASCs pushes the iris until angle contact due to PC enlargement [34]. Increased angulation or bulging of the iris caused by ASCs is related to an increase in IOP. These findings suggest narrow of the ACA and closure of the AOA as a risk factor for CAG [5]. Iridociliary ASCs can be discriminated on SLBM by angulation of the iris. Usually, they can be displayed with dilatation and gonioscopy. Patients can be suspected of having ASCs due to positive transillumination [34]. UBM is superior for the evaluation of iridociliary structures, and it provides real-time, high-resolution diagnostic images of the closure of the ACA in patients with ASCs who are at risk of CAG [23,32]. Moreover, multiple small cysts detected by UBM could indicate one large and additional multiple small ASCs in the iridociliary area.

Most ASCs can simply be monitored without requiring treatment [2,35]. Making an early and cross-sectional diagnosis allows for well-adapted treatment [36]. The treatment of ASCs should provide an effective AOA and pupillary aperture, and should involve excision of the cellular layer as well as ablation therapy to eradicate proliferative residual cells in excised ASC sites [37]. Recurrence and severe complications can occur after surgery. Postoperative OHT might be related to obstacles in the outflow pathway, trabecular insufficiency, iris incarceration, or conjunctival scarring [5,13]. Eyes with glaucoma have significant anatomic differences from normal eyes. The most significant clinical hallmarks are the shallow AL, ACD and narrow angle [15]. AL and ACD are widely evaluated to eliminate the possibility of primary glaucoma or related conditions [23].

In recent studies, associations have been reported between the IOP and UBM features of ASCs, including size, shape, and location [6]. Iridociliary ASCs are relatively large and have an impressed and deformed shape, with extension into the pupillary aperture [10]. ASCs can cause complications such as

visual axis narrowing, closure of the ACA-AOA, and iridocorneal decompensation [13,31]. The more involved area of iris the more increased IOP, compatible with literature [13,35]. When ASCs enlarge, they project between the iris and anterior lens capsule into the pupillary region [5,35]. Secondary CAG can occur in patients with large ASCs due to pushing against the iris, increasing intracavitary secretion, inflammation, and uveitis [31].

Many identification and imaging techniques for management of the anterior segment have been reported [14,38]. SLBM, gonioscopy, pentacam, UBM, and OCT are imaging techniques that allow evaluation of the anterior-segment, SLBM and gonioscopy are currently the gold standard imaging techniques assessing anterior-segment, while pentacam measures corneal pachymetry and visualises the effects of an increased IOP on the anterior-segment [15,39]. OCT provides high-resolution imaging of the central iris hump, but it fails to evaluate the PC and iridociliary region because of lower signal penetration [3,40]. Pentacam measures corneal pachymetry and the ACA-AOA [41]. Thus, these imaging modalities serve to complement gonioscopy. Van Herick grading system is widely used to assess ACA-AOA [18]. UBM, as a cross-sectional imaging technique with high interobserver variability, is useful for analysing the AC and PC because of greatly attenuated signals within the PC and ciliary body, and provides cross-sectional imaging of the anterior-segment, cornea, iridociliary junction, and ciliary body lesions, which are undetectable by SLBM [6,16,32]. Combining various imaging modalities could strengthen the diagnosis and management of ASCs [19].

This was a hospital-based cross-sectional, retrospective study with a limited number. Data were not collected systematically, so it may have been prone to selection bias because we recruited participants with ASCs. Additionally, we did not analyse the effect of treatment on the ACA-AOA in patients with ASCs.

In conclusion, it was shown previously that ASCs might cause CAG and that there is a relationship between closure of the ACA and increased IOP. In our study, the ACA was found to be significantly narrowed in OHT compared to the ONT group, and significant correlations were demonstrated between the degree of closure of the ACA and increased IOP associated with UBM parameters, including etiology, location, shape, size of the ASCs and pupillary aperture. The integration of imaging modalities strengthens the management of OHT in patients with ASCs. We may like to comment on which of these parameters using these instruments would most useful to aware and monitor change in these ASCs over time. Additional studies are needed to clarify the complex relationship between an increased IOP in patients with ASCs, as a risk factor for CAG.

Acknowledgements: We wish to thank Gwendolyn Mack, Imaging Science, University of Rochester, for her dedicated contributions in graphics.

**REFERENCES**

- 1 Shields JA, Kline MW, Augsburger JJ. Primary iris cysts a review of the literature and report of 62 cases. *Br J Ophthalmol* 1984;68(3):152–166
- 2 Grutzmacher RD, Lindquist TD, Chittum ME, Bunt–Milan AH, Kalina RE. Congenital iris cysts. *Br J Ophthalmol* 1987;71(3):227–234
- 3 Pong JC, Lai JS. Imaging of primary cyst of the iris pigment epithelium using anterior segment OCT and ultrasonic biomicroscopy. *Clin Exp Optom* 2009;92(2):139–141
- 4 Krohn J, Hove VK. Recurring iris pigment epithelial cyst induced by topical prostaglandin F2 alpha analogues. *Arch Ophthalmol* 2008;126(6):867–868
- 5 Haller JA, Stark WJ, Azab A, Thomsen RW, Gottsch JD. Surgical management of anterior chamber epithelial cysts. *Am J Ophthalmol* 2003;135(3):309–313
- 6 Marigo FA, Esaki K, Finger PT, Ishikawa H, Greenfield DS, Liebmann JM, Ritch R. Differential diagnosis of anterior segment cysts by ultrasound biomicroscopy. *Ophthalmology* 1999;106(11):2131–2135
- 7 Miki A, Saishin Y, Kuwamura R, Ohguro N, Tano Y. Anterior segment optical coherence tomography assessment of iris bombé before and after laser iridotomy in patients with uveitic secondary glaucoma. *Acta Ophthalmol* 2010;88(2):26–27
- 8 Baykara M, Sahin S, Ertürk H. Free iris cyst in the anterior chamber. *Ophthalmic Surg Lasers Imaging* 2004;35(1):74–75
- 9 Donate D, Kodjikian L, Gambrelle, Buriollon C, Denis P. Buphthalmia secondary to congenital pigmented epithelial iris cyst. *J Fr Ophthalmol* 2004;27(5):496–500
- 10 Behrouzi Z, Ramezani A. Precipitate inside the epithelial iris cyst a report of two cases. *Graefe's Arch Clin Exp Ophthalmol* 2007;245(1):176–178
- 11 Zhou C, Qian S, Yao J, Tang Y, Qian J, Lu Y, Xu G, Sun X. Clinical analysis of 50 Chinese patients with aqueous misdirection syndrome: a retrospective hospital–based study. *J Int Med Res* 2012;40(4):1568–1579
- 12 Xiao Y, Wang YH, Niu GL, Gao M. Primary Iris Stromal Cyst with Rapid Growth. *Optom Vis Sci* 2009;86(11):1309–1312
- 13 Honda N, Mimura T, Hotehama A, Usui T, Sugisaki K, Fukuoka S, Amano S. Laser treatment of giant iris cyst with nanophthalmos. *Int Ophthalmol* 2011;31(1):17–20
- 14 Buchwald H–J, Spraul CW, Wagner P, Lang GK. Ultrasound biomicroscopy in iris lesions. *Ophthalmologe* 1999;96(2):108–113
- 15 Sihota R, Dada T, Aggarwal A, Srinivasan G, Gupta V, Chabra VK. Does an iridotomy provide protection against narrowing of the anterior chamber angle during Valsalva manoeuvre in eyes with primary angle closure. *Eye* 2008;22(3):389–393
- 16 Tello C, Liebmann J, Potash SD, Cohen H, Ritch R. Measurement of ultrasound biomicroscopy images: intraobserver and interobserver reliability. *Invest Ophthalmol Vis Sci* 1994;35(9):3549–3552
- 17 Dorairaj S, Liebmann JM, Ritch R. Quantitative evaluation of anterior segment parameters in the era of imaging. *Trans Am Ophthalmol Soc* 2007;105:99–110
- 18 Park SB, Sung KR, Kang SY, Jo JW, Lee KS, Kook MS. Assessment of narrow angles by gonioscopy, Van Herick method and anterior segment optical coherence tomography. *Jpn J Ophthalmol* 2011;55(4):343–350
- 19 Ursea R, Silverman RH. Anterior–segment imaging for assessment of glaucoma. *Expert Rev Ophthalmol* 2010;5(1):59–74
- 20 Pavlin CJ, Foster FS. Plateau iris syndrome: changes in angle opening associated with dark, light, and pilocarpine administration. *Am J Ophthalmol* 1999;128(3):288–291
- 21 Ishikawa H, Liebmann JM, Ritch R. Quantitative assessment of the anterior segment using ultrasound biomicroscopy. *Curr Opin Ophthalmol* 2000;11(2):133–139
- 22 Console JW, Sakata LM, Aung T, Friedman DS, He M. Quantitative analysis of anterior segment optical coherence tomography images the Zhongshan Angle Assessment Program. *Br J Ophthalmol* 2008;92(12):1612–1616
- 23 Nolan W. Anterior segment imaging: ultrasound biomicroscopy and anterior segment optical coherence tomography. *Curr Opin Ophthalmol* 2008;19(2):115–121
- 24 Jiang Y, He M, Huang W, Huang Q, Zhang J, Foster PJ. Qualitative assessment of ultrasound biomicroscopic images using standard photographs: the liwan eye study. *Invest Ophthalmol Vis Sci* 2010;51(4):2035–2042
- 25 Potash SD, Tello C, Liebmann J, Ritch R. Ultrasound biomicroscopy in pigment dispersion syndrome. *Ophthalmology* 1994;101(2):332–339
- 26 Kumar RS, Baskaran M, Chew PT, Friedman DS, Handa S, Lavanya R, Sakata LM, Wong HT, Aung T. Prevalence of plateau iris in primary angle closure suspects an ultrasound biomicroscopy study. *Ophthalmology* 2008;115(3):430–434
- 27 Bron AJ, Wilson CB, Hill AR. Laser treatment of primary ring–shaped epithelial iris cyst. *Br J Ophthalmol* 1984;68(12):859–865
- 28 Xu L, Cao WF, Wang YX, Chen CX, Jonas JB. Anterior chamber depth and chamber angle and their associations with ocular and general parameters: the Beijing Eye Study. *Am J Ophthalmol* 2008;145(5):929–936
- 29 Shin HC, Subrayan V, Tajunisah I. Changes in anterior chamber depth and intraocular pressure after phacoemulsification in eyes with occludable angles. *J Cataract Refract Surg* 2010;36(8):1289–1295
- 30 Sallo FB, Hatvani I. Recurring transitory blindness caused by primary marginal pigment epithelial iris cysts. *Am J Ophthalmol* 2002;133(3):407–409
- 31 Alward WL, Ossoinig KC. Pigment dispersion secondary to cysts of the iris pigment epithelium. *Arch Ophthalmol* 1995;113(12):1574–1575
- 32 Dada T, Gadia R, Sharma A, Ichhpujani P, Bali SJ, Bhartiya S, Panda A. Ultrasound biomicroscopy in glaucoma. *Surv Ophthalmol* 2011;56(5):433–450
- 33 Gupta V, Rao A, Sinha A, Kumar N, Sihota R. Post–traumatic inclusion cysts of the iris: a longterm prospective case series. *Acta Ophthalmol Scand* 2007;85(8):893–896
- 34 Le Corre A, Dot C, Feraoun M, Burelle X, Grasswill C, Perrenoud F, May F. Plateau iris–like configuration resulting from numerous iridociliary cysts. *J Fr Ophthalmol* 2009;32(7):501–504
- 35 Augsburger JJ, Affel LL, Benarosh DA. Ultrasound Biomicroscopy of cystic lesions of the iris and ciliary body. *Am J Ophthalmol* 1996;94:259–274
- 36 Crowston JG, Medeiros FA, Mosaed S, Weinreb RN. Argon laser iridoplasty in the treatment of plateau–like iris configuration as result of numerous ciliary body cysts. *Am J Ophthalmol* 2005;139(2):381–383
- 37 Chan RY, Pong JC, Yuen HK, Lai JS. Use of sodium hyaluronate and indocyanine green for conjunctival cyst excision. *Jpn J Ophthalmol* 2009;53(3):270–271
- 38 See JL. Imaging of the anterior segment in glaucoma. *Clin Experiment Ophthalmol* 2009;37(5):506–513
- 39 Friedman DS, He M. Anterior chamber angle assessment techniques. *Surv Ophthalmol* 2008;53(3):250–273
- 40 Mansouri K, Sommerhalder J, Shaarawy T. Prospective comparison of ultrasound biomicroscopy and anterior segment optical coherence tomography for evaluation of anterior chamber dimensions in European eyes with primary angle closure. *Eye* 2010;24(2):233–239
- 41 Chou CY, Jordan CA, McGhee CN, Patel DV. Comparison of intraocular pressure measurement using 4 different instruments following penetrating keratoplasty. *Am J Ophthalmol* 2012;153(3):412–418